BEAM DYNAMICAL CALCULATIONS WITH REALISTIC FIELDS IN A DRIFT TUBE LINEAR ACCELERATOR*

Marvin Rich
University of California, Los Alamos Scientific Laboratory
Los Alamos, New Mexico

Summary

A method for numerical beam dynamics studies of drift tube type linear accelerators using electromagnetic fields similar to those encountered in actual machines is presented. Results of calculations for a 90 mev accelerator are given and comparisons made with similar calculations in which the axial electric field is assumed spatially constant within the accelerating gap.

I. Introduction

Although linear accelerators have been designed successfully using simplified approximations to the accelerating fields and to the solutions for the particle motion, there is still interest in determining what differences may occur when relatively close approximations are made to the electromagnetic fields and to the motion of the particles. In this paper we would like to describe a numerical procedure for beam dynamics calculations of drift tube type linear accelerators in which the axial electric field is spatially parabolic within the gap and zero within the drift tubes. This is an extension of some previously reported work[1] in which the axial field within the gap was assumed spatially constant. The procedure consists of two parts: (a) the calculation of the off axis electromagnetic fields within the gap as a power series in the radial coordinate, r, using Maxwell's equations and the assumed axial electric field, and (b), the construction of an approximate solution to the motion of a charge particle within these fields. The method stands in contrast with the more usual approach to numerical beam dynamics in which only the principle harmonic of the accelerating field is used, and its effect upon a particle approximated by an impulse applied at the center of a gap.

In Section II, the equations for the electromagnetic fields which have been used within an accelerating gap and the approximate solution to the particle motion are presented. Some results of an application of these equations to the study of a 90 mev linear accelerator are given in Section III. These calculations have been made both with uniform axial fields and with parabolic fields programmed to simulate the variation in field shape with increasing energy in order to ascertain what, if any, differences result.

II. The Computational Method

The Electromagnetic Field

The calculation of the accelerating fields which have been used in the computations to be presented is based on the assumption that the longitudinal electric field has the following form on the accelerator axis:

$$E_z(r=0,z) = E_0\theta(z+\tfrac{g}{2})\ \theta(\tfrac{g}{2}-z)f(z) \qquad \tfrac{L}{2} \le z \le \tfrac{L}{2} \quad (1)$$

where

$$f(z) = 1 - \frac{4R}{g^2} z^2 \quad (2)$$

Here L is the distance between drift tube centers and g is the length of the accelerating gap as shown in Fig. 1. R is one minus the ratio of field strength at the gap edge to that at the gap center. The step function $\theta(x)$ is unity for positive x and zero for negative x. This field configuration may be considered periodic with period L.

The off axis fields can be obtained easily by writing the solution of Maxwell's equations for a harmonically varying periodic configuration with cylindrical symmetry in terms of Fourier-Bessel series:

$$E_z(r,z,t) = E_0 \sum_{n=0}^{\infty} a_n \cos\frac{2n\pi z}{L}\, I_0(b_n r)\cos\omega t$$

$$E_r(r,z,t) = -E_0 \sum_{n=0}^{\infty} \frac{a_n}{b_n}\frac{2n\pi}{L}\sin\frac{2n\pi z}{L}\, I_1(b_n r)\cos\omega t$$

$$B_\theta(r,z,t) = -\frac{\omega}{c^2} E_0 \sum_{n=0}^{\infty} \frac{a_n}{b_n}\cos\frac{2n\pi z}{L}\, I_1(b_n r)\sin\omega t$$

where ω is the angular frequency of the oscillating field and

$$b_n = \sqrt{\left(\frac{2\pi n}{L}\right)^2 - \left(\frac{\omega}{c}\right)^2}$$

Expanding the Bessel functions in powers of r and resumming the series with the aid of the relation

$$\theta(z+\tfrac{g}{2})\ \theta(\tfrac{g}{2}-z)\ f(z) = \sum_{n=0}^{\infty} a_n \cos\frac{2n\pi z}{L}$$

gives, through third order in r,

$$E_z = E_0\left\{\theta(z+\tfrac{g}{2})\theta(\tfrac{g}{2}-z)f(z) + \frac{r^2}{4}s(z)\right\}\cos\omega t$$

$$E_r = -E_0\left\{\frac{r}{2}\left[\delta(z+\tfrac{g}{2})f(z) - \delta(z-\tfrac{g}{2})\ f(z)\right]\right.$$

(continued)

$$+ \frac{r}{2}\,\theta(z+\tfrac{g}{2})\theta(\tfrac{g}{2}-z)\,\frac{df(z)}{dz} + \frac{r^3}{16}\,\frac{ds(z)}{dz}\Big\}\cos\omega t$$

$$B_\theta = -E_0\,\frac{\omega}{c^2}\Big\{\frac{r}{2}\,\theta(z+\tfrac{g}{2})\theta(\tfrac{g}{2}-z)f(z) + \frac{r^3}{16}\,s(z)\Big\}\sin\omega t \tag{3}$$

with

$$s(z) = -\left(\frac{\omega^2}{c^2} + \frac{d^2}{dz^2}\right)[\theta(z+\tfrac{g}{2})\theta(\tfrac{g}{2}-z)f(z)] \tag{4}$$

Approximate Solution to the Equations of Motion

The Cartesian equations of motion for a particle moving in a cylindricaly symmetric electromagnetic field are

$$\frac{du_i}{dt} = \frac{e}{m}\left[E_r - \frac{u_s}{\gamma}B_\theta\right]\frac{x_i}{r} \qquad i = 1,2$$

$$\frac{du_3}{dt} = \frac{e}{m}\left[E_z + \frac{u_1x_1 + u_2x_2}{\gamma r}B_\theta\right] \tag{5}$$

$$\frac{dx_i}{dt} = u_i/\gamma \qquad i = 1,2,3 \tag{6}$$

where indices 1, 2, and 3 correspond to the x, y, and z directions, respectively, $r = (x_1^2 + x_2^2)^{1/2}$, and $\gamma = (1 + \vec{u}^2/c^2)^{1/2}$.

Because of the appearance of δ-function and their derivatives in the fields at the gap extremities, $z = \pm g/2$, a particle will receive both a radial and a longitudinal impulse upon entering or leaving a gap. These δ-function contributions simulate the effects of the rapid rise of the off-axis electromagnetic fields necessitated by the sudden reduction of the fields on entering a drift tube. Neglecting small terms, the impulse received by a particle entering a gap is approximately

$$\Delta u_i = -\frac{E_0}{2}\frac{e}{m}x_i\frac{\gamma}{u_3}\left\{f(z)\left(1 + \frac{r^2}{8}\frac{\omega^2}{u_3^2}\right)\cos\omega t - \frac{r^2}{8}\left(\frac{df(z)}{dz}\sin\omega t + \frac{\omega}{\gamma u_3}\frac{d^2f(z)}{dz^2}\cos\omega t\right)\right\} \tag{7}$$

$$i = 1,2$$

$$\Delta u_3 = -E_0\frac{e}{m}\frac{r^2}{4}\left\{\frac{df(z)}{dz}\cos\omega t + f(z)\frac{\omega\gamma}{u_3}\sin\omega t\right\}$$

where the coordinates, time, and u-components are those at the arrival of the particle at the gap. Similar impulses, with opposite overall signs, occur on leaving the gap.

Within the gap, the fields to be used in Eqs. (5) and (6) are

$$E_z = E_0\left\{\left(1 - \frac{r^2}{4}\frac{\omega^2}{c^2}\right)f(z) - \frac{r^2}{4}\frac{d^2f(z)}{dz^2}\right\}\cos\omega t$$

$$E_r = -\frac{r}{2}E_0\left\{\left(1 - \frac{r^2}{8}\frac{\omega^2}{c^2}\right)\frac{df(z)}{dz} - \frac{r^2}{8}\frac{d^3f(z)}{dz^3}\right\}\cos\omega t$$

$$B_\theta = -\frac{r}{2}\frac{\omega}{c^2}E_0\left\{\left(1 - \frac{r^2}{8}\frac{\omega^2}{c^2}\right)f(z) - \frac{r^2}{8}\frac{d^2f(z)}{dz^2}\right\}\sin\omega t$$

A relatively simple and accurate approximation to the particle motion within the gap can be obtained by inserting linearly time dependent forms for the position coordinates occurring in the above field:

$$x_i = x_i^{(0)} + \frac{u_i^{(0)}}{\gamma_0}t \qquad i = 1,2$$

$$x_3 = -\frac{g}{2} + \bar{v}\,t$$

where the zeros refer to the particle parameters immediately after entering the gap and the velocity $\bar{v}$ is the gap length, g, divided by the time required for the particle to cross the gap. Again omitting small terms and assuming that the particle enters the gap at time t = 0, the equations of motion can now be integrated to give

$$\begin{aligned} u_i(t) = u_i^{(0)} + \frac{e}{m}\frac{E_0}{\omega}g\Bigg\{&\frac{4R}{g^2}\left(1 - \frac{r_0^2}{8}\frac{\omega^2}{c^2}\right)\Bigg[x_i^{(0)} \\ &\times\left(\frac{\sin\psi + \sin\psi_0}{2} + \frac{\cos\psi - \cos\psi_0}{\omega t}\right) \\ &+ \frac{u_i^{(0)}}{\omega\gamma_0}\left(\frac{\omega t}{2}\sin\psi + \frac{3\cos\psi + \cos\psi_0}{2}\right. \\ &\left.+ \frac{2(\sin\psi - \sin\psi_0)}{\omega t}\right)\Bigg] - \frac{1}{2}\frac{\omega^2}{c^2}x_i^{(0)} \\ &\times\left[1 - \frac{r_0^2}{8}\frac{\omega^2}{c^2} + \frac{r_0^2R}{g^2}\right]\frac{(\cos\psi - \cos\psi_0)}{\omega t}\Bigg\} \end{aligned} \tag{8}$$

$$i = 1,2$$

$$\begin{aligned} u_3(t) = u_3^{(0)} + \frac{e}{m}\frac{E_0}{\omega}\left(1 - \frac{r_0^2}{4}\frac{\omega^2}{c^2}\right)\Bigg\{&\left[1 - R\left(1 - \frac{8}{(\omega t)^2}\right)\right] \\ &\times(\sin\psi - \sin\psi_0) - 4R\,\frac{\cos\psi + \cos\psi_0}{\omega t}\Bigg\} \end{aligned} \tag{9}$$

(continued)

$$+ \frac{e}{m}\frac{E_0}{\omega}\left\{\frac{2r_0^2R}{g^2}(\sin\psi - \sin\psi_0) + \frac{u_1^{(0)}x_1^{(0)} + u_2^{(0)}x_2^{(0)}}{\omega\gamma_0}\frac{4R}{g^2} \times (\cos\psi - \cos\psi_0 + \omega t\sin\psi_0)\right\}$$

$$x_i(t) = x_i^{(0)} + \frac{u_i^{(0)}}{\gamma_0}t + \frac{e}{m}\frac{E_0}{\omega^2\gamma_0}g\left\{\frac{4R}{g^2}\left(1 - \frac{r_0^2}{8}\frac{\omega^2}{c^2}\right) \times \left[x_i^{(0)}\left(\frac{\omega t}{2}\sin\psi_0 - \frac{\cos\psi + 3\cos\psi_0}{2} + \frac{2(\sin\psi - \sin\psi_0)}{\omega t}\right) + \frac{u_i^{(0)}}{\omega\gamma_0}\left(\left(\frac{6}{\omega t} - \frac{\omega t}{2}\right) \times (\cos\psi - \cos\psi_0) + 3(\sin\psi + \sin\psi_0)\right)\right] - \frac{1}{2}\frac{\omega^2}{c^2}x_i^{(0)}\left[1 - \frac{r_0^2}{8}\frac{\omega^2}{c^2} + \frac{r_0^2R}{g^2}\right] \times \left(\frac{\sin\psi - \sin\psi_0}{\omega t} - \cos\psi\right)\right\} \quad i = 1,2 \tag{10}$$

$$x_3(t) = -\frac{g}{2} + \frac{u_3^{(0)}}{\gamma_0}t - \frac{e}{m}\frac{E_0}{\omega^2\gamma_0}\left(1 - \frac{u_3^{(0)2}}{c^2\gamma_0^2}\right) \times \left(1 - \frac{r_0^2}{4}\frac{\omega^2}{c^2}\right)\left\{\left[1 - R\left(1 - \frac{24}{(\omega t)^2}\right)\right] \times (\cos\psi - \cos\psi_0) + (1-R)\omega t\sin\psi_0 + 4R\left[\cos\psi_0 + \frac{2}{\omega t}(\sin\psi + 2\sin\psi_0)\right]\right\} - \frac{e}{m}\frac{E_0}{\omega^2\gamma_0^2}\left(1 - \frac{u_3^{(0)2}}{c^2\gamma_0^2}\right)\left\{\frac{2r_0^2R}{g^2} \times (\cos\psi - \cos\psi_0 + \omega t\sin\psi_0) + \frac{u_i^{(0)}x_1^{(0)} + u_2^{(0)}x_2^{(0)}}{\omega\gamma_0}\frac{4R}{g^2} \times [\omega t(\cos\psi + \cos\psi_0) - 2(\sin\psi - \sin\psi_0)]\right\} \tag{11}$$

In these equations ψ_0 is the phase of the electromagnetic field when the particle centers the gap and $\psi = \omega t + \psi_0$.

A Beam Dynamics Code

Although Eqs. (8) through (11) appear considerably more formidable than equations more commonly employed in numerical beam dynamics studies, their use does not result in excessive increases in computation time compared to simpler, less accurate procedures. The beam dynamics code which has been written using these equations consists of two parts. In the first, the accelerator geometry is computed given the stable phase, the energy gain per unit length, and the g/L and field shape sequences for each tank. From the stable phase, ψ_{stable}, and the g/L ratio, the phases of the electromagnetic field at which the axial design particle is required to enter and leave the n^{th} gap are specified to be

$$\psi_{in}(n) = \psi_{stable} - \pi(g/L)_n$$
$$\psi_{out}(n) = \psi_{stable} + \pi(g/L)_n \tag{12}$$

The length of the n^{th} gap can then be calculated from Eq. (11) using the requirement that, with $x_{1,2}^{(0)} = 0$, $x_3(t) = g_n/2$ when $\omega t = \psi_{out}(n) - \psi_{in}(n)$:

$$g_n = \frac{u_3^{(0)}}{\omega\gamma_0}\omega t - \frac{e}{m}\frac{E_0}{\omega^2\gamma_0^3}\left\{\left[1 - R\left(1 - \frac{24}{(\omega t)^2}\right)\right] \times (\cos\psi_{out} - \cos\psi_{in}) + (1-R)\omega t\sin\psi_{in} + 4R\left[\cos\psi_{in} + \frac{2}{\omega t}\sin\psi_{out} + 2\sin\psi_{in})\right]\right\} \tag{13}$$

If u_n is the longitudinal "momentum" of the design particle at the end of the n^{th} gap as obtained from Eq. (9)

$$u_n = u_3^{(0)} + \frac{e}{m}\frac{E_0}{\omega}\left\{\left[1 - R\left(1 - \frac{8}{(\omega t)^2}\right)\right](\sin\psi_{out} - \sin\psi_{in}) - 4R\frac{\cos\psi_{out} + \cos\psi_{in}}{\omega t}\right\}, \tag{14}$$

then the length of the n^{th} drift tube will be

$$l_n = \left(\psi_{in}(n+1) - \psi_{out}(n) + 2\pi\right)\left(1 + u_n^2/c^2\right)^{-\frac{1}{2}}u_n/\omega \tag{15}$$

The field strength, E_0, to be used with the n^{th} gap equations is determined from the energy gain per unit length, ϵ, by

$$E_0(n) = \epsilon(g/L)_n^{-1}\int_{-g/2}^{g/2}dz\bigg/\int_{-g/2}^{g/2}E_z(0,z,t)\,dz = \epsilon(g/L)_n^{-1}\left[\psi_{out}(n) - \psi_{in}(n)\right]$$

(continued)

$$\times \left\{ \left[1 - R\left(1 - \frac{8}{\omega t^2}\right) \right] (\sin \psi_{out} - \sin \psi_{in}) - 4R \, \frac{\cos \psi_{out} + \cos \psi_{in}}{\omega t} \right\}^{-1} \tag{16}$$

where again $\omega t = \psi_{out}(n) - \psi_{in}(n)$.

Following the specification of the accelerator geometry, assignment is made of a quadrupole magnet configuration and of possible sets of random quadrupole and gap field errors and misalignment errors.

In the second part of the code, particles with various initial phase, energy, and off-axis position and velocity are carried through the structure using Eqs. (8) through (11). The time required to cross a gap is found first by solving Eq. (11) for ωt with $x_3(t) = g/2$:

$$\begin{aligned}
\omega t = \Bigg\{ & g + \frac{e}{m} \frac{E_0}{\omega^2 \gamma_0} \left(1 - \frac{u_3^{(0)2}}{c^2 \gamma_0^2}\right) \left[\left(1 - \frac{r_0^2}{4} \frac{\omega^2}{c^2}\right) \right. \\
& \times \left\{ \left[1 - R\left(1 - \frac{24}{(\omega t)^2}\right) \right] (\cos \psi - \cos \psi_0) + 4R \right. \\
& \left. \times \left[\cos \psi_0 + \frac{2}{\omega t} (\sin \psi + 2 \sin \psi_0) \right] \right\} + \frac{2 r_0^2 R}{g^2} \\
& \times (\cos \psi - \cos \psi_0) + \frac{u_1^{(0)} x_1^{(0)} + u_2^{(0)} x_2^{(0)}}{\omega \gamma_0} \frac{4R}{g^2} \\
& \left. \times \left[\omega t (\cos \psi + \cos \psi_0) - 2(\sin \psi - \sin \psi_0) \right] \right\} \\
& \times \Bigg\{ \frac{u_3^{(0)}}{\omega \gamma_0} - \frac{e}{m} \frac{E_0}{\omega^2 \gamma_0} \left(1 - \frac{u_3^{(0)2}}{c^2 \gamma_0^2}\right) \\
& \times \left[\left(1 - \frac{r_0^2}{4} \frac{\omega^2}{c^2}\right)(1 - R) - \frac{2 r_0^2 R}{g^2} \right] \sin \psi_0 \Bigg\}^{-1}
\end{aligned} \tag{17}$$

Solution of this equation is obtained by iteration starting with an initial guess of $\omega t_0 = \psi_{out}(n) - \psi_{in}(n)$. For an accuracy of one part in 10^5, two iterations are generally required with a third iteration being necessary in a few percent of the gaps. Substitution of the time found by Eq. (17) into Eqs. (8), (9) and (10) yields the final radial position and the velocity preceding the final impulse. Transit through quadrupole magnets within the drift tubes is accomplished by the usual linear approximation.[2]

III. Some Comparative Design Studies for a 90 Mev Accelerator

The computing method described above has been used in an attempt to determine what differences in the computed phase and radial motion will occur for an accelerator of given design specifications when parabolic axial field shapes are prescribed in contrast to constant fields. In addition, as a test of accuracy, a comparison was made of the phase motion with parabolic fields between results using Eqs. (9) and (11) and a direct integration of the equations of motion to carry particles through the same accelerator configuration. For both problems, an errorless 90 Mev accelerator of interest in the L.A.S.L. design program was considered, specifications for which were

Tank	1	2	3
Final Energy (Mev)	8	50	90
Energy gain/meter (Mev/m)	1.11	1.75	1.32
g/L range	0.20 to 0.28	0.18 to 0.30	0.33 to 0.40
Drift space (m)	0.30	0.9144	

The injection energy was 0.75 Mev and the operating frequencies and "stable phases" were chosen to be 201.25 Mc and -26°, respectively, for all three tanks. Quadrupole magnets were assumed to occupy 55% of the length of each drift tube with a sequence of + - + - in the first tank and 0 + 0 - thereafter. The initial quadrupole strength was taken to be 6100 gauss/cm and was programmed to decrease as $1/\beta$. Finally, for parabolic fields, the shape parameter R was chosen to be the following function of design particle energy as determined from a fit to calculated gap fields[3] at 10, 50, and 100 Mev:

$$R = 0.19667 - 0.0203\, E + 6.333 \cdot 10^{-5}\, E^2$$

In the comparison with the numerical integration of the equations of motion, phase and energy oscillation amplitudes with respect to the design particle were found to be in agreement within a few tenths of one percent, except at the limiting edges of the acceptance region where some differences of the order of one percent occurred.

The comparison of calculations with the parabolic and the constant gap fields did not reveal any appreciable differences. The geometries of the accelerators designed with the two field forms were identical everywhere to five significant figures, and were determined solely by the prescribed energy gain per meter, g/L sequence, and stable phase. As a consequence of this, the phase-energy acceptance fishes differed almost imperceptibly for the two cases. Figure 2 shows the phase-energy acceptance region, applicable to both field types, and also three curves giving the emittance in terms of phase and energy oscillation coordinates for fixed initial energy and varying initial phase. Some of the initial phases are indicated on the 0.75 Mev emittance curve. The range of initial phases and energies was chosen to enclose that portion of the acceptance fish appropriate to a typical buncher. The maximum amplitudes of the phase and energy oscillations of this group of particles are seen to be about 6° and 0.5 Mev, respectively.

Differences in the radial motion between the parabolic and uniform field calculations was also small. The structure of the radial oscillations was essentially the same for both cases, with radial displacements differing by at most 5%. Although the radial impulses received by a particle at the extremities of a gap in the parabolic field computations generally differed greatly from those in the constant field case, the radial force within the gap was such as to cause the net motion to remain similar to that with uniform gap fields. The extent of these differences can be seen in Figure 3 where the radial acceptance for a particle with the design energy and phase is shown. The solid lines refer to the acceptances with parabolic axial fields. The circles and x's indicate the acceptance region for calculations with constant axial fields. The cut-off at a radius of one centimeter is due to an assumed one centimeter radius hole in drift tubes in the first tank. Calculated acceptances were about 31π mrad.-cm in both the x-z and y-z planes.

*Work done under the auspices of the U.S. Atomic Energy Commission.

References

1. M. Rich: Proceedings of the 1964 MURA Linear Accelerator Conference.

2. Smith and Gluckstern: Rev. Sci. Instr., 26, 220 (1955).

3. M. Rich and W. M. Visscher: Proceedings of the 1964 MURA Linear Accelerator Conference.

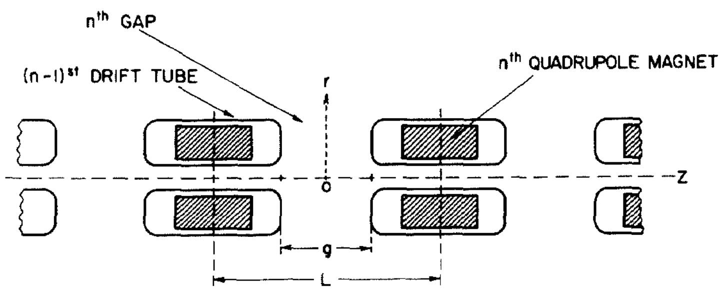

Fig. 1. Schematic diagram of a drift tube section.

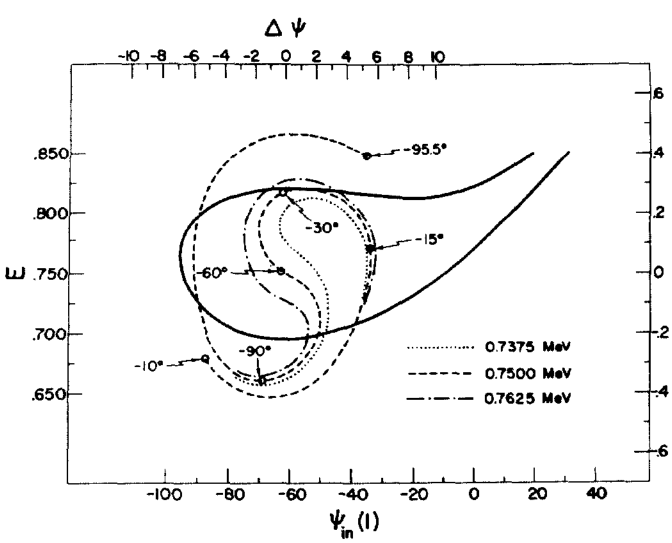

Fig. 2. Calculated phase-energy acceptance and emittance of a 90 Mev linear accelerator, using parabolically shaped gap fields. Energies are in Mev and phases in degrees.

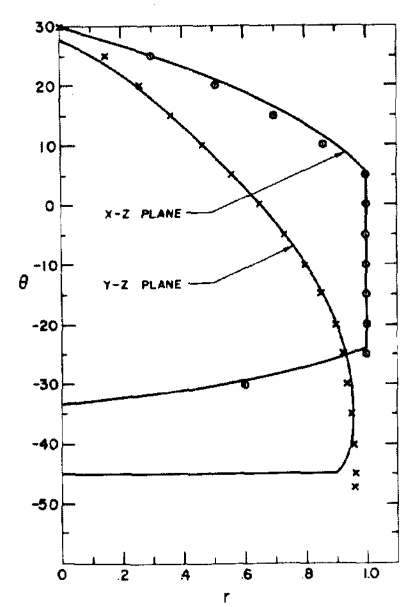

Fig. 3. Radial acceptance for particles of initial energy of 0.75 Mev and initial phase $\psi_{in}(1) = -62°$. Angles are in milli-radians and radii in centimeters. Solid lines refer to computations with parabolic axial gap fields. Circles and x's refer to computations with constant axial fields.